Synthetic and Systems Biotechnology 9 (2024) 285–293

Contents lists available at ScienceDirect

Synthetic and Systems Biotechnology

journal homepage: www.keaipublishing.com/en/journals/synthetic-and-systems-biotechnology

Original Research Article

Multi-modular metabolic engineering of heme synthesis in *Corynebacterium glutamicum*

Qiuyu Yang [a,b,1], Xi Sun [a,b,1], Hong Wang [a,b], Tao Chen [a,b], Zhiwen Wang [a,b,c,*]

[a] Frontier Science Center for Synthetic Biology and Key Laboratory of Systems Bioengineering (Ministry of Education), Tianjin University, Tianjin, 300072, China
[b] SynBio Research Platform, Collaborative Innovation Center of Chemical Science and Engineering (Tianjin), School of Chemical Engineering and Technology, Tianjin University, Tianjin, 300072, China
[c] School of Life Science, Ningxia University, Yinchuan, 750021, China

ARTICLE INFO

Keywords:
Corynebacterium glutamicum
Heme
Biosynthetic pathways
Metabolic engineering

ABSTRACT

Heme, an iron-containing porphyrin derivative, holds great promise in fields like medicine, food production and chemicals. Here, we developed an engineered *Corynebacterium glutamicum* strain for efficient heme production by combining modular engineering and RBS engineering. The whole heme biosynthetic pathway was methodically divided into 5-ALA synthetic module, uroporphyrinogen III (UPG III) synthetic module and heme synthetic module for further construction and optimization. Three heme synthetic modules were compared and the siroheme-dependent (SHD) pathway was identified to be optimal in *C. glutamicum* for the first time. To further improve heme production, the expression of genes in UPG III synthetic module and heme synthetic module was coordinated optimized through RBS engineering, respectively. Subsequently, heme oxygenase was knocked out to reduce heme degradation. The engineered strain HS12 showed a maximum iron-containing porphyrin derivatives titer of 1592 mg/L with the extracellular secretion rate of 45.5% in fed-batch fermentation. Our study constructed a *C. glutamicum* chassis strain for efficient heme accumulation, which was beneficial for the advancement of efficient heme and other porphyrins production.

1. Introduction

Heme is an iron-containing porphyrin derivative that consists of a porphyrin macrocycle and a ferrous ion, which serves as a cofactor for enzymes involved in a wide range of physiological reactions in organisms [1]. Heme has found extensive application in the field of medicine as an effective iron supplement and as a treatment for triple-negative breast cancer when combined with metformin [2]. Hemin containing chloride ions has demonstrated potential in the management of acute intermittent porphyria [3]. In addition, heme plays a role as a food additive in the synthesis of artificial meat [4], and it serves as raw material for semi-synthetic hematoporphyrin and sodium protoporphyrin in fine chemicals process [5]. Recent studies have uncovered promising applications of heme in biochemical analysis and biocatalysts [6]. Along with the wide range of applications and high value of heme, efficient production of heme has become an urgent requirement.

Currently, heme is conventionally derived through chemical synthesis or extraction from plant tissues and animal blood [7,8]. Due to the complexity and pollution of these methods, the microbial synthesis of heme has attracted much attention from researchers. In microbial pathway, heme can be synthesized from the precursor substrate 5-aminolevulinic acid (5-ALA), with uroporphyrinogen III (UPG III) as the key intermediate metabolite [9]. 5-ALA can be obtained from glycine or glutamine via the C4 or C5 pathway [10]. The eight 5-ALA molecules then undergo a strictly conserved three-enzyme pathway to form the first cyclic molecule, UPG III [5]. The porphyrin ring or side chain of UPG III was modified using the protoporphyrin-dependent (PPD) pathway, coproporphyrin-dependent (CPD) pathway or siroheme-dependent (SHD) pathway to ultimately produce heme. The PPD pathway was found in eukaryotes and many Gram-negative bacteria, while the CPD pathway primarily observed in Gram-positive bacteria, and they are both known as the classical heme synthetic

Peer review under responsibility of KeAi Communications Co., Ltd.
* Corresponding author. Frontier Science Center for Synthetic Biology and Key Laboratory of Systems Bioengineering (Ministry of Education), Tianjin University, Tianjin, 300072, China.
E-mail address: zww@tju.edu.cn (Z. Wang).
[1] These authors contributed equally to this work.

https://doi.org/10.1016/j.synbio.2024.02.008
Received 22 December 2023; Received in revised form 19 February 2024; Accepted 28 February 2024
Available online 6 March 2024

pathways [11]. The SHD pathway was considered to be an evolutionarily conserved pathway in sulfate-reducing bacteria and Archaea [12], which has not been used for the synthesis of heme in bacteria.

In 2003, Kwon et al. [13] made the first attempt to reconstruct the heme biosynthetic pathway in *E. coli* by employing three compatible plasmids containing genes from the C4 and PPD pathways. This construct allowed heme production to 3.3 μmol/L, confirming the possibility of microbial heme synthesis. Zhao et al. [14] constructed an *E. coli* strain HAEM7 using the C5 pathway and the optimized PPD pathway for heme biosynthesis. Following further optimization of the fermentation process, a heme titer of 1.03 g/L was obtained with the productivity of 21.5 mg/L/h [15]. *Corynebacterium glutamicum*, as a famous amino acids industrial producer with GRAS (generally regarded as safe) status [16], has been extensively engineered for the production of variety of commercially interesting compounds [17,18]. Recent studies have expanded its capabilities to include the production of heme [19], hemoglobin [20] and the major precursors of heme, such as 5-ALA [21,22] and biliverdin [23]. A growth-coupled, high-throughput selection platform was developed for improving heme biosynthesis [24]. Ko et al. [19] combined the C4 and C5 pathways for precursor 5-ALA production, and co-overexpressed *dtxR* and genes of CPD pathway. The engineered strain exhibited a maximum heme titer of 309.18 mg/L. Although the global transcriptional regulator DtxR showed a positive effect on heme accumulation in *C. glutamicum* [25,26], the intricate regulatory mechanism of heme biosynthetic pathway in *C. glutamicum* remained unclear [22]. This resulted in an inherently low activity of the key enzymes, which limited the overproduction of heme. As previously mentioned, the heme synthetic SHD pathway has not been utilized for heme synthesis in prokaryotic cells. Among all the CPD pathway, PPD pathway and SHD pathway, which was more suitable for heme synthesis in *C. glutamicum* remained unclear. In addition, the precise modulation of the relative expression intensity of genes was also imperative for efficient heme synthesis.

In this study, a rapidly carbon-utilizing chassis CGS15 was used for heme production [27]. The overall heme synthetic pathway was divided into three modules, the 5-ALA synthetic module, the UPG III synthetic module and the heme synthetic module. Firstly, various sources of AlaS and their mutants were screened to ensure an ample supply of 5-ALA precursors. Secondly, CPD pathway, PPD pathway and SHD pathway were constructed in *C. glutamicum* to identify the most efficient heme synthetic pathway. Then, RBS engineering was used to fine-tune the relative expression levels of genes in the UPG III synthetic module and the heme synthetic module, respectively. Subsequently, heme accumulation was further promoted by blocking the competitive pathways and overexpressing genes of the heme transporter. Finally, fed-batch fermentations were performed for scalable production of heme. The *C. glutamicum* platform strains HS12 produced 1592 mg/L of total iron-containing porphyrin derivatives (ICPDs) with 725 mg/L secreted ICPDs, which indicated that *C. glutamicum* holds promise to be a potential microbial cell factory to produce heme effectively.

2. Materials and methods

2.1. Media and culture conditions

LB medium consisting of 5 g/L yeast extract, 10 g/L tryptone, and 10 g/L NaCl was used for cloning all target genes in *E. coli* DH5α. BHI medium consisting of 74 g/L brain heart infusion was used for cloning of all engineered vectors in *C. glutamicum* and the preculture of all engineered strains. Modified CGIII complex medium (pH 7.4) containing of 10 g/L tryptone, 10 g/L yeast extract, 21 g/L 3-morpholinopropanesulfonic acid (MOPS) and 2.5 g/L NaCl was used for flask cultivations. The initial glucose concentration was 30 g/L. Isopropyl β-D-1-thiogalactopyranoside (IPTG) (1 mM), glycine (7.5 g/L) and $FeSO_4{\cdot}7H_2O$ (20 mg/L) were added at 6, 8 and 12 h of flask cultivation respectively. Kanamycin (40 mg/L for *E. coli* and 25 mg/L for *C. glutamicum*) and chloramphenicol (10 mg/L for *E. coli* and 5 mg/L for *C. glutamicum*) were added to the medium when appropriate.

Flask cultivations for 5-ALA and heme production were performed as follows. All wild-type and engineered strains, stored at a cryogenic temperature, were streaked on BHI agar plates and cultured for 36 h at 30 °C. The cultured cells were inoculated in 5 mL BHI liquid medium and incubated at 30 °C and 200 rpm for 12 h. Then, 1 mL of the seeds were inoculated into 250 mL baffled flask containing 50 mL of CGIII medium and incubated at 30 °C, 220 rpm for 12 h. Finally, the cultures with an initial optical density OD_{600} of 0.5 were inoculated into 250 mL shake flasks containing 50 mL CGIII medium at 30 °C, 200 rpm for 48 h.

Fed-batch fermentations for heme production were performed in a 5 L fermenter with 2 L fresh fermentation medium. Modified CGXII (CGXIIY) medium (pH 7.0) containing (per liter): yeast extract 15 g, $(NH_4)_2SO_4$ 20 g, urea 5 g, KH_2PO_4 1 g, K_2HPO_4 1 g, $MgSO_4{\cdot}7H_2O$ 0.25 g, $CaCl_2$ 10 mg, $FeSO_4{\cdot}7H_2O$ 10 mg, $MnSO_4{\cdot}H_2O$ 0.1 mg, $ZnSO_4{\cdot}7H_2O$ 1 mg, $CuSO_4{\cdot}5H_2O$ 0.2 mg, $NiCl_2{\cdot}6H_2O$ 20 μg, biotin 0.2 mg and MOPS 21 g was used for fed-batch fermentations. The 200 mL seed culture was inoculated into the fermenter containing 1.7 L CGXIIY medium supplemented with 30 g/L of glucose. 1 mM IPTG was added at 6 h, 7.5 mg/L glycine was added at 8 h, 200 mg/L $FeSO_4{\cdot}7H_2O$ was added at 12 h. Fermentation was carried out at 30 °C. Ammonium hydroxide and HCl were used to maintain pH at 7.0. The minimum dissolved oxygen was maintained at 40% air saturation for the first 8 h, and then that was maintained at 20% air saturation. The feed solution containing 800 g/L glucose was added automatically to maintain the glucose concentration below 5 g/L.

2.2. Construction of plasmids and strains

The recombinant plasmids and strains used in this study are listed in Supplementary Table 1. The RBS sequences used for plasmid library construction were listed in Supplementary Table 2. The genomic DNA of *C. glutamicum* was used to amplify the *hemE*, *hemF*, *hemY*, *hemH*, *hemQ*, *hrtB*, *hrtA*, *hrrS*, *hmuT* and *htaA* genes. To construct the complete SHD pathway, genes *SYNTR-0459*, *SYNTR-0456*, *SYNTR-1652*, *SYNTR-0463* and *SYNTR-0460* from *Candidatus syntrophocurvum alkaliphilum* were synthesized and codon-optimized by Azenta (Suzhou, China). pEC-XK99E and pXMJ19 vectors were used as shuttle vectors for *E. coli* and *C. glutamicum* for the overexpression of target genes. The genetic modification of *C. glutamicum* was achieved via a two-step homologous recombination procedure using the suicide vector pD-sacB.

The target fragments were amplified by polymerase chain reaction (PCR) and inserted into the plasmid by T4 DNA ligase (Thermo Fisher Fermentas) or seamless cloning kit (US EVERBRIGHT). Plasmid libraries are constructed using the Golden Gate Assembly Kit (BsaI-HF®v2). To achieve efficient assembly between fragments, primers used in this study were designed by https://goldengate.neb.com/#!/(Supplementary Table 3). All experiments for recombinant vector construction were performed according to the manufacturer's instructions. Then, each ligation mixture was transformed into competent *E. coli* DH5a cells. The transformation of the recombinant vectors into *C. glutamicum* was performed as previously described [27].

2.3. Analytical methods

Growth was monitored by measuring the optical density at 600 nm (OD_{600}) using a conventional spectrophotometer (TU-1901, PUXI, Beijing, China). The concentration of glucose in the fermentation broth was determined using HPLC. The chromatographic column was HPX-87H (Bio-rad), and the mobile phase was 5 mM H_2SO_4 at a flow rate of 0.5 mL/min. The sample injection volume was set at 10 μL, and the temperature of the column oven was set at 60 °C. ALA was measured using the colorimetric assay called Ehrlich's reagent [26]. To extract heme, 1 mL of fermentation broth was centrifuged at 12,000 rpm for 5 min at 4 °C, and the extracellular supernatant was separated. After

separating supernatant, 1 mL acidic acetone buffer (95:5 ratio of 99% acetone:1.6 M HCl) was added to the extract the cell pellet. After vertexing for approximately 30 s, the sample was centrifuged at 12,000 rpm, 4 °C for 5 min to obtain intracellular supernatants. ICPDs was measured by fluorescence assay as described previously [22]. The heme content was measured by HPLC analysis as described previously [15].

2.4. High-throughput screening for efficient heme-producing strains

The fermentation broth of the constructed strain was used as a sample to detect the intracellular heme concentration and the fluorescence intensity of sirohydrochlorin. The fluorescence intensity of sirohydrochlorin was measured at the excitation wavelength of 375 nm and the emission wavelength of 670 nm by a Varioskan LUX fluorescence microplate reader (Thermo Fisher Scientific, CA, USA). In order to screen the high fluorescence intensity strains, the Golden Gate multi-fragment plasmid library was electrically transferred into SH0 strain. Then, the mixed bacterial system was screened in PerCP-Cy5-5-5-A (488 nm, 695/40 nm) channel by Flow Cytometer (BD Aria III, USA), and single cell with high fluorescence intensity were obtained for plate culture.

2.5. Real-time quantitative PCR (RT-qPCR)

The total RNA extraction and reverse transcription to synthesize cDNA were performed as described. Briefly, total RNA was extracted using the RNeasy Mini Kit (Qiagen, Valencia, CA, USA) and cDNA synthesis was carried out using the TransScript® First-Strand cDNA Synthesis SuperMix (Transgen Corp. Beijing, China). the TransStart® Top Green qPCR SuperMix (TransGen, Beijing, China) on a LightCycler® 480 device (Roche, Basel, Switzerland) was used to amplify and quantify the PCR of the products. Primers for RT-PCR used in this study were listed in Supplementary Table 4. The transcriptional level of the 16S ribosomal RNA served as the internal reference. Both the targeted genes and test strains were subjected to triplicate replicates.

3. Results and discussion

3.1. Modular design of the heme synthetic pathway

Heme can be synthesized from the precursor substrate 5-ALA, with UPG III as the key intermediate metabolite in *C. glutamicum*. Here, the complex heme biosynthetic pathway was divided into three modules for separate construction and optimization (Fig. 1). In the first module, named the 5-ALA synthetic module, the C4 pathway was employed to synthesize 5-ALA from succinyl-CoA in a single step, by utilizing the pyridoxal-5′-phosphate (PLP)-dependent ALA synthase (AlaS) [10]. In the second module, named the UPG III synthetic module, the intermediate metabolite UPG III was synthesized by a conserved core pathway [5]. Two 5-ALA molecules were catalyzed by porphobilinogen synthase

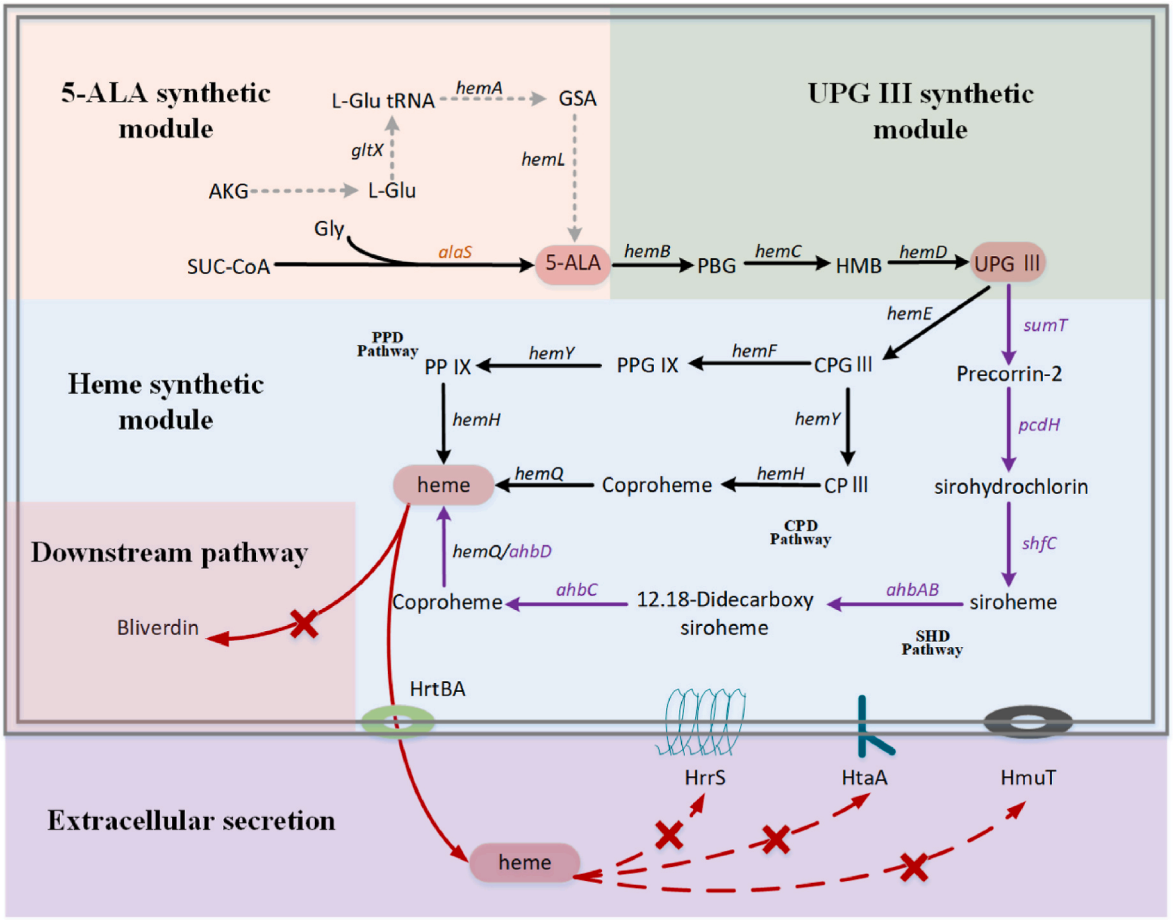

Fig. 1. Schematic overview describing the target pathway and overall metabolic strategies for heme production. The entire pathway is divided into three parts: 5-aminolevulinic acid (5-ALA) biosynthetic pathway (orange), uroporphyrinogen III (UPG III) biosynthetic pathway (green) and heme biosynthetic pathway (blue). There are three different pathways of heme biosynthesis in organisms. Abbreviations: OAA, oxaloacetate; MAL, malate; FUM, fumarate; SUC, succinate; SUC-COA, succinyl-CoA; α-KG, α-oxoglutarate; GLY, glycine; GLU, glutamate; GLU-tRNA, glutamyl-tRNA; GSA, glutamate-1-semialdehyde; 5-ALA, 5-aminolevulinic acid; PBG, porphobilinogen; HMB, hydroxymethylbilane; UPG I, uroporphyrinogen I; CPG I, coproporphyrinogen I; UPG III, uroporphyrinogen III; CPG III, coproporphyrinogen III; PPG IX, protoporphyrinogen IX; PP IX, protoporphyrin IX; CP III, coproporphyrin III.

(HemB), hydroxymethylbilane synthase (HemC) and uroporphyrinogen synthase (HemD) to form UPG III [28–30]. In the final module, named the heme synthetic module, three distinct pathways were explored for heme synthesis. The PPD pathway with four consecutive enzymatic reactions, the CPD pathway with three consecutive enzymatic reactions and the SHD pathway with a six-step reaction were compared for heme synthesis.

3.2. Construction and optimization of the 5-ALA synthetic module

Ensuring a sufficient 5-ALA supply is crucial for effective heme synthesis. AlaS is a key enzyme of 5-ALA synthetic pathway, which is inhibited by tight feedback inhibition from heme at multiple levels of protein hydrolysis [31]. Heme could bind to AlaS through the cysteine of AlaS to form a heme-ALAS complex which may represse the activity of AlaS [32,33]. Site-directed mutation of cysteines in AlaS has been proved to be a powerful strategy to interrupt the interaction of ALAS with heme to release heme inhibition of AlaS in our previous study [34]. The AlaS from *Rhodopseudomonas palustris* and *Rhodobacter capsulatus* and their cysteine mutants were compared in *C. glutamicum* for 5-ALA synthesis, and $AlaS_{RP}^{C132A}$ and $AlaS_{RC}^{C210A}$ were proved to be able to significantly alleviate the inhibitory effect of high concentrations of heme on AlaS.

To assess the capacity of heme synthesis of these AlaS mutants, the pEC-XK99E (medium copy number) plasmid was utilized to overexpress $alaS_{RP}$, $alaS_{RP}^{C132A}$, $alaS_{RC}$ and $alaS_{RC}^{C210A}$ in CGS15, yielding the engineered strains A1, A2, A3 and A4, respectively. As shown in Fig. 2a, the introduction of AlaS significantly increased the production of 5-ALA. The mutant strain A2 with $alaS_{RP}^{C132A}$ exhibited the highest 5-ALA concentration of 3.57 ± 0.36 g/L, which was 1.4-fold higher than that of strain A1 (2.60 ± 0.26 g/L). Mutant strain A4 with $alaS_{RC}^{C210A}$ also showed a 1.7-fold increase in 5-ALA production compared with strain A3 (2.60 ± 0.31 g/L versus 1.54 ± 0.22 g/L). The total ICPDs concentration of the engineered strains A1 (17.1 ± 1.6 mg/L), A2 (17.1 ± 1.2 mg/L), A3 (14.6 ± 1.9 mg/L) and A4 (19.1 ± 1.6 mg/L) increased compared with strain CGS15 (11.9 ± 1.97 mg/L). However, the ICPDs concentration of A2 and A4 did not show a sharp increase compared with A1 and A3 as expected, respectively (Fig. 2b). This may be due to the current 5-ALA concentration was excessive, and the activities of key enzymes of UPG III synthetic module and heme synthetic module are not sufficient to convert 5-ALA to other intermediate metabolites. Therefore, the UPG III synthetic module and heme synthetic module were further engineered to improve heme production. Given the highest 5-ALA production achieved by overexpressing the $alaS_{RP}^{C132A}$ gene, the mutant strain A2 was selected for the following metabolic engineering.

3.3. Construction of UPG III synthetic module and heme synthetic module

UPG III is an important nodal metabolite for the conversion of 5-ALA to heme, and most prokaryotes have the ability to synthesize UPG III from scratch [11]. Therefore, the native *hemB*, *hemC* and *hemD* were overexpressed using the *trc* promoter to construct strain BCDA2 (Fig. 3a). The ICPDs concentration of BCDA2 reached 252.0 ± 9.4 mg/L including 128.1 ± 6.25 mg/L of secreted ICPDs, which was 17.7-fold higher than that of the A2 (Fig. 3b). The maximum accumulation of 5-ALA of BCDA2 correspondingly decreased to 1.74 ± 0.09 g/L (Fig. 3c). Notably, the maximum biomass of BCDA2 and A2 was significantly decreased compared with CGS15 (Supplementary Fig. 1, 19.7 versus 20.4 versus 23.3). It has been reported that when heme accumulation was increased, the expression of genes of glucose transport, glycolysis, respiratory chain and ATP synthesis were down-regulated, and the transcription of genes involved in oxidative stress and protein repair were up-regulated [22]. These facts offered a plausible explanation for the reduced growth capacity of BCDA2 and A2.

There are three heme synthetic pathways exist in organisms, of which the PPD pathway was frequently utilized for construction and optimization in *E. coli* [11,13], the CPD pathway was mostly applied in *C. glutamicum* [22,23] and the SHD pathway was commonly found in sulfate-reducing bacteria and Archaea [35]. To determine the most efficient pathway for the heme synthetic module, these three pathways were overexpressed and compared in BCDA2. Genes of PPD pathway and CPD pathway were obtained from *C. glutamicum* ATCC 13032, genes of SHD pathway, *pcdH*, *shfC*, *ahbAB* and *ahbC* were sourced from *Candidatus syntrophocurvum alkaliphilum* [36]. To minimize the additional metabolic burden of exogenous genes on the host, the gene of the first step of SHD pathway was replaced by *cgl1998* and the gene of the final step of SHD pathway was replaced by *hemQ* from *C. glutamicum*. To avoid additional metabolic burden, strain HP, HC and HS were constructed based on BCDA2 strain by overexpressing PPD, CPD and SHD pathways, respectively, with medium copy number plasmid pXMJ19. (Fig. 3a).

HS with the heterologous SHD pathway totally produced 288 ± 9.2 mg/L ICPDs with a secretion rate of 57.3%, which was 14.3% higher than BCDA2 (Fig. 3b). The 5-ALA content of HS was further decreased to 0.38 ± 0.03 g/L (Fig. 3c), suggesting that more 5-ALA was converted to heme. Unexpectedly, HP and HC strains showed reduced ICPDs production capacity (Fig. 3b) and virtually no 5-ALA accumulation (Fig. 3c). This may be due to that the native CPD pathway and PPD pathway were subject to strict feedback inhibition. As reported, overexpression of *hemY, hemH* and *hemQ* led to a decrease in heme production and specific growth rate in *C. glutamicum* ATCC 14067 [19]. The HemY protein catalyzed the generation of H_2O_2, which triggering the regulation of genes associated with oxidative stress and protein repair to adapt to the increased H_2O_2 [22,37]. Additionally, the HemH protein

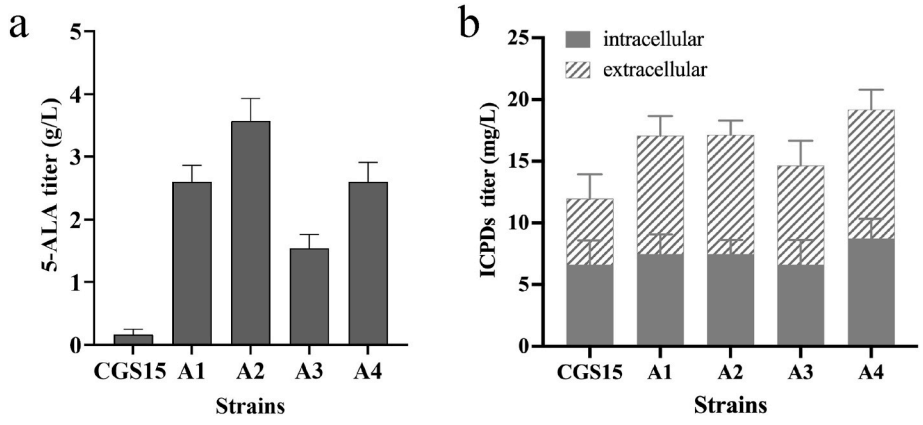

Fig. 2. Construction and optimization of the 5-ALA synthetic module in *C. glutamicum*. (a) 5-ALA and (b) ICPDs production of strains with different AlaS.

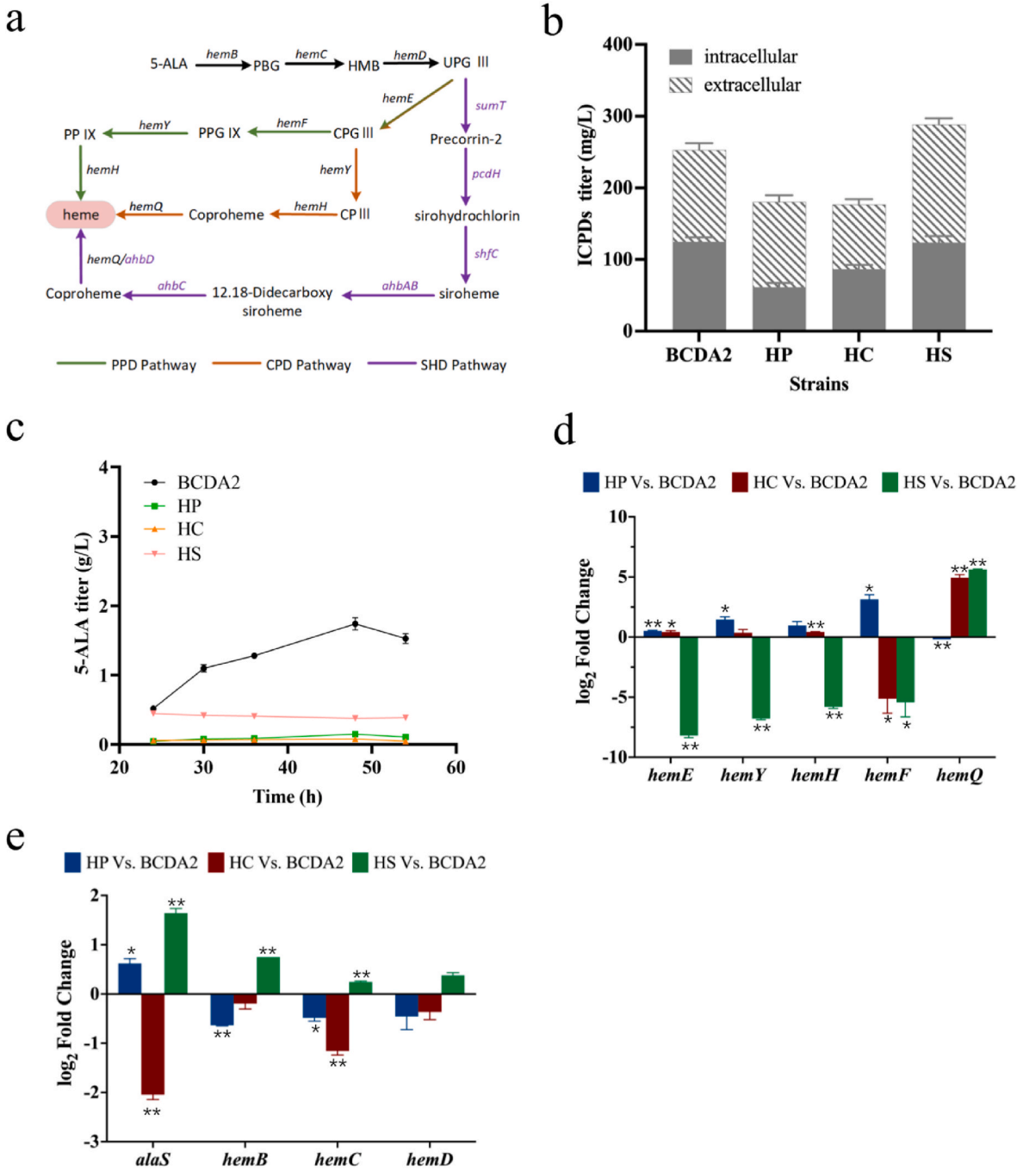

Fig. 3. Construction of UPG III synthetic module and heme synthetic module in *C. glutamicum*. a, three heme biosynthetic pathways used in this study. ICPDs (b) and 5-ALA (c) production of BCDA2, HP, HC and HS. Transcriptional level changes of genes related to heme synthetic module (d), the 5-ALA synthetic module and UPG III synthetic module (e) according to qRT-PCR. Error bars indicate the standard deviations from three independent replicates. Single and double asterisks indicated p values of <0.05 and < 0.01, respectively.

used iron to synthesize copro-heme and the iron metabolism is tightly regulated to maintain iron-heme homeostasis [19,25]. The transcription of other genes related to heme metabolism in the *hemH* overexpressing strain was decreased. Collectively, these facts suggested that perturbation of the CPD pathway in *C. glutamicum* caused global regulatory changes [19]. Thus, the exogenous SHD pathway was identified as the optimal heme synthetic pathway in *C. glutamicum*. Therefore, we determined the expression of genes in 5-ALA synthetic module, UPG III synthetic module and heme synthetic module of the BCDA2, HP, HC and HS strain. Although *hemE, hemY* and *hemH* genes were overexpressed in HP and HC, the expression of these genes was not significantly higher in HP and HC than that in BCDA2 (Fig. 3d). While, the expression of the *hemQ* was increased more than 30-fold in HC and HS (Fig. 3d). This suggests that *hemQ*, unlike genes such as *hemE, hemY* and *hemH*, was not very tightly regulated. Interestingly, *alaS* of HC was significantly down-regulated and genes involved in UPG III synthetic module of HP and HC (Fig. 3e). This may explain the absence of 5-ALA accumulation in HP and HC. Conversely, the expression of genes in 5-ALA synthetic module and UPG III synthetic module of HS were increased compared to BCDA2 strain (Fig. 3e). Overexpression of the exogenous SHD pathway simultaneously inhibits the expression of the endogenous heme synthesis pathway. This could lead to an increased carbon flux toward the

SHD pathway. Thus, the exogenous SHD pathway was identified as the optimal heme synthetic pathway in *C. glutamicum*.

3.4. Optimization of gene expression in the UPG III synthetic module by RBS engineering

Overexpression of target product synthetic pathways often disrupts the internal microbial self-balance, resulting in significant imbalances in pathway fluxes [21]. Fine-tuning at the translational level through ribosome binding site (RBS) engineering particularly effective for the optimization of multigene combinatorial expression. To further enhance the heme production capacity of engineered strains, the expression of genes in the UPG III synthetic module was co-optimized by RBS engineering. A total of 16 RBS sequences in *C. glutamicum* were collected from the available literature and their translation rate values were calculated using the RBS Calculator (Supplementary Table 2). Among the RBSs with similar translation rate, one RBS was selected for the subsequent screening. 8 RBSs with varying translation intensities were selected and characterized with green fluorescent protein (Fig. 4a). To ensure differential expression intensity, RBS5, RBS1, RBS2 and RBS11 with different intensity gradients were selected to construct the RBS library. As shown in Fig. 4b, each plasmid contained *hemB*, *hemC* and *hemD* genes that were independently regulated by RBS of different strengths. The theoretical library size was 4^3.

To establish a high-throughput screening method for efficient heme-producing strains, we sought to indirectly assess the intracellular ICPDs concentration by measuring the fluorescence intensity of sirohydrochlorin [38]. The relative fluorescence intensity of sirohydrochlorin exhibited a consistent trend with the intracellular ICPDs content (Supplementary Fig. 2). Consequently, cells with strong fluorescence signals were sorted by flow cytometry, enabling high-throughput screening for heme high-producing strains.

The plasmid library and the pX-SHD plasmid were introduced into A2, simultaneously. Cells were screened by flow cytometry, resulting in the selection of 152 single colonies with notably high fluorescence intensity. These colonies underwent further fermentation to validate their heme production capabilities. The highest total ICPDs concentration reached to 337.0 ± 11.6 mg/L, which was 17% higher than that of strain HS, and the secretion rate was 53.2% (Fig. 4c). The strain exhibiting the highest total ICPDs concentration, named HS2, was then sequenced. The optimal RBS combination of the *hemB*, *hemC* and *hemD* genes was proved to be RBS11-RBS2-RBS11.

3.5. Optimization of gene expression in the heme synthetic module by RBS engineering

The SHD pathway of the heme synthetic module involves six genes: *sumT*, *pcdH*, *shfC*, *ahbAB*, *ahbC* and *hemQ*. To identify the key targets for efficient heme production, the RBS of the six genes were replaced with strong RBS, respectively, constructed strain HS3-HS8 (Fig. 5a). As shown in Fig. 5b, HS8 with overexpression of *hemQ* showed the highest ICPDs concentration of 343.2 ± 10.6 mg/L, which was only 6 mg/L higher than that of HS2 (337.0 ± 11.6 mg/L). Notably, the extracellular secretion rate of strain HS8 overexpressing *hemQ* gene increased to 67%, which was 1.26-fold compared to that of strain HS2 (53.2%). The *hemQ* gene has been previously demonstrated to be a key target gene for heme synthesis in *C. glutamicum* and *B. subtilis* when using the CPD pathway [19,39]. Our findings suggested that the *hemQ* gene also plays an important role in the production of heme by SHD pathway. Unexpectedly, the ICPDs production of HS3 (284.3 ± 10.2 mg/L), HS4 (294.4 ± 11.3 mg/L) and HS5 (287.9 ± 9.5 mg/L) was slightly decreased and that of HS6 (193.3 ± 10.3 mg/L) and HS7 (186.4 ± 8.3 mg/L) was significantly decreased (Fig. 5b). This may be due to the toxic effect of the overaccumulation of intermediate metabolites during the enhanced expression of the single gene, which inhibited the production of the target product. Therefore, it was hypothesized that *ahbAB* and *ahbC* need to be weakly expressed.

To further engineer the SHD pathway, RBS with relatively high (H, RBS11), medium (M, RBS2), or low (L, RBS1) strength was selected for the six genes. According to the previous description, a relatively low level of the expression of *ahbAB* and *ahbC* was found to be advantageous for the efficient production of heme. Therefore, based on the high expression of *hemeQ*, three RBS combinations were designed to construct the strain HS9, HS10 and HS11 (Fig. 5c). Strain HS10, with the combination of $sumT^{M}$, $pcdH^{M}$, $shfC^{M}$ $ahbAB^{L}$, $ahbC^{L}$ and $hemeQ^{H}$, displayed the highest ICPDs concentration of 391 mg/L with an extracellular secretion rate of 59.6%. Compared to HS2, the ICPDs production of HS10 was increased by 16% and the secretion rate of ICPDs was increased by 12% (Fig. 5c). Unexpectedly, the ICPDs production of strains with $sumT^{H}$, $pcdH^{H}$ and $shfC^{H}$ was not enhanced (HS9 and HS11,

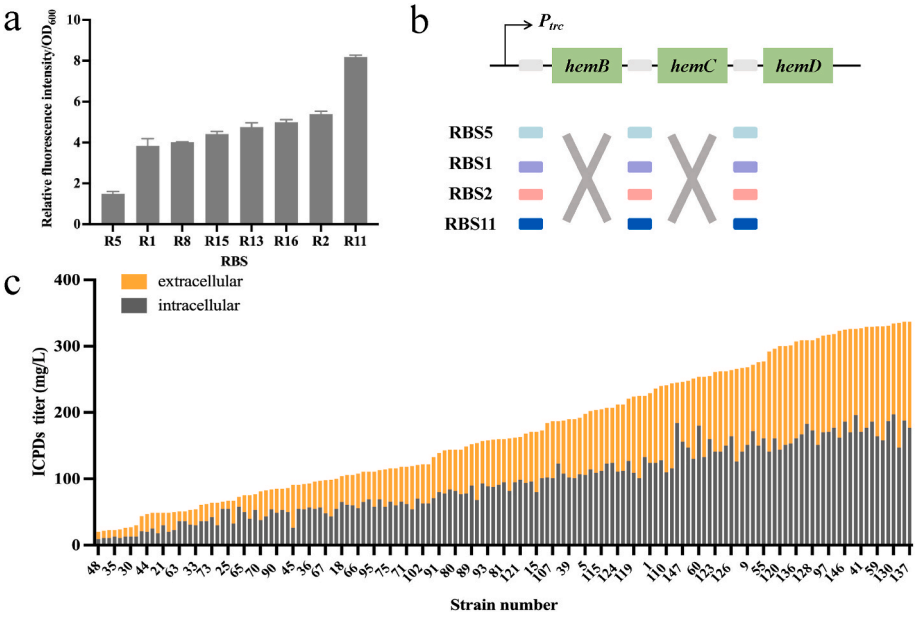

Fig. 4. Optimization of gene expression in the UPG III synthetic module. (a) Fluorescence characterization of RBS with different intensities. (b) Structure diagram of plasmid library. (c) ICPDs production of screened strains.

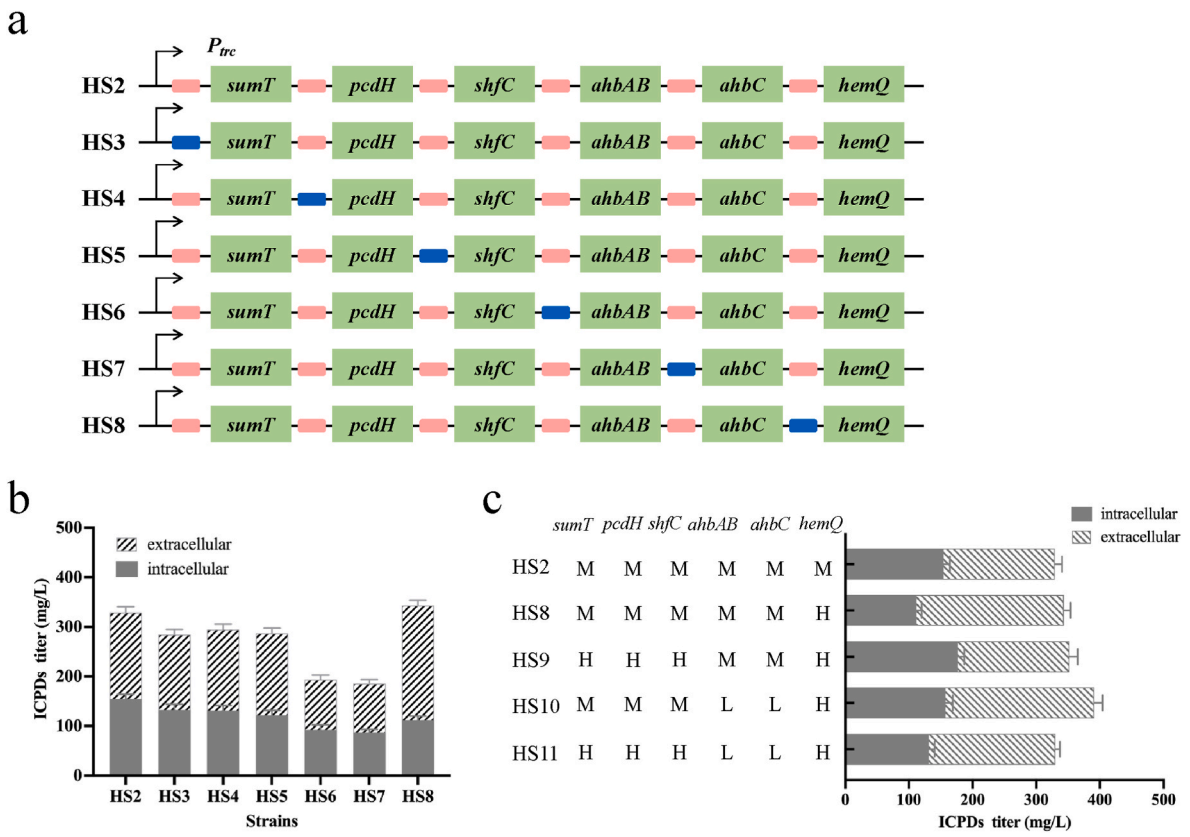

Fig. 5. Combinatorial optimization of heme synthetic module. (a) Schematic diagram of construction of single gene RBS enhanced strains in the SHD pathway. Red is medium strength RBS2 and blue is high strength RBS11. (b) Effect of single gene enhancement on ICPDs production in heme synthetic module. (c) Effect of gene combination optimization of heme synthetic module on ICPDs production. Blue represents high strength RBS11, pink represents moderate strength RBS2, and purple represents low strength RBS1.

353.1 ± 10.4 mg/L and 330.8 ± 7.6 mg/L). This implied that increasing the supply of the intermediate metabolite siroheme had a negative impact on heme production. It could be speculated that heme metabolism might be regulated by the intermediate metabolites of SHD pathway, which needs to be further investigated.

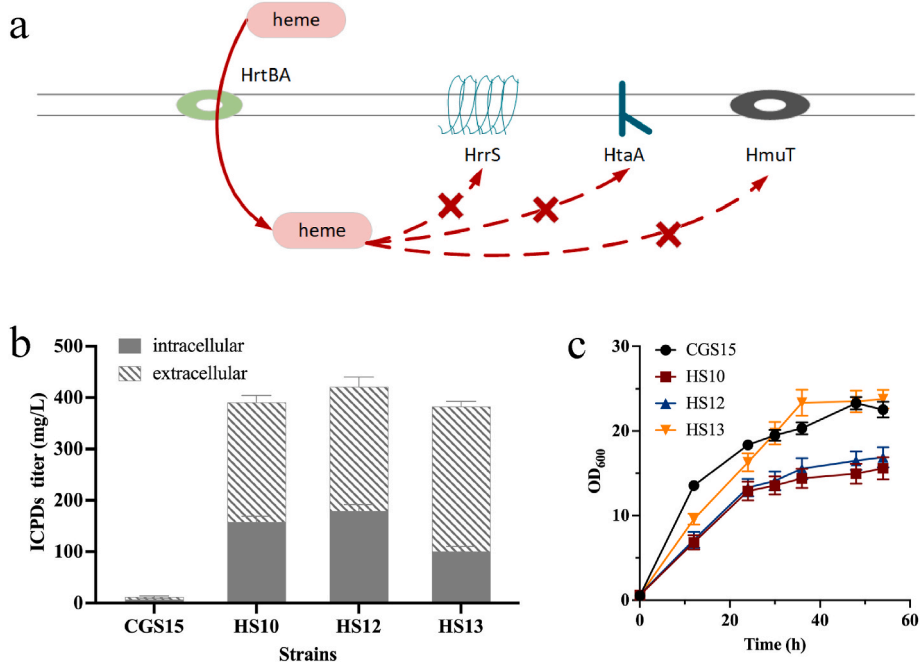

Fig. 6. Culture results of genetically engineered strains related to blocking downstream pathways and disturbing heme secretion. a, schematic diagram of heme secretion pathway. Effects of blocking downstream pathways and interfering with heme secretion-related genes on ICPDs titers (b) and growth (c).

3.6. Engineering of heme downstream pathways and secretion

As reported, *C. glutamicum* can utilize heme as an alternative source of iron, with heme oxygenase (HmuO, encoded by the *cgl2227* gene) as the primary enzyme [25]. Heme oxygenase catalyzes the degradation of heme to biliverdin, carbon monoxide and free iron. Therefore, it is necessary to knockout *hmuO* to reduce heme degradation (Fig. 6a). The ICPDs production of HS12, knocking out *hmuO*, reached 421.3 ± 12.4 mg/L, increased by 7.6% compared to HS10. The ICPDs secretion rate of HS12 was 57.5%, which was similar to that of HS10 (Fig. 6b). Moreover, the maximum biomass of HS12 was slightly increased compared with HS10 (Figs. 6c and 16.5 versus 14.95).

To mitigate the potential toxicity associated with an excessive intracellular heme concentration, it was imperative to focus on metabolic engineering modifications related to heme transport. Heme transporter protein A (HrtA, encoded by the *cgl1784* gene) and heme transporter protein B (HrtB, encoded by the *cgl1782* gene) have been identified to be involved in heme secretion [19]. Meanwhile, HrrS (encoded by the *cgl2937* gene), HtaA (encoded by the *cgl0388* gene) and HmuT (encoded by the *cgl0389* gene) proteins are typical heme-binding membrane proteins in *C. glutamicum* which are responsible for the uptake of exogenous heme as an iron source [25,40,41]. To reduce extracellular heme uptake and enhance the secretion of intracellular heme, the *htaA* and *hmuT* were replaced with *hrtA* and *hrtB* and the *hrrS* gene was knockout in HS12, resulting the strain HS13 (Fig. 6a). The ICPDs extracellular secretion rate of HS13 reached to 73.9%, which was the highest secretion rate of all constructed strains. Unfortunately, the total ICPDs concentration of HS13 was 382.5 ± 9.8 mg/L, which was lower than that of HS12 (Fig. 6b). The maximum biomass of HS13 was significantly increased compared with HS10 and HS12 (Fig. 6c). *HrrS* was the component of HrrSA two-component system which plays a crucial role in maintaining the homeostasis of heme, integrating the response to oxidative stress and cell envelope remodeling [42–44]. It was hypothesized that the knockout of *hrrS* may impact the function of HrrSA system and cause complex effects on heme production and cell growth. Considering the decreased heme production capacity of HS13, HS12 with knocking out *hmuO*, which showed the highest heme titer in a shake flask, was employed for scale fermentations.

3.7. Fed-batch fermentation for heme in 5 L fermenter

For scale production of heme, a fed-batch fermentation of HS12 was performed in a 5 L fermenter with 2 L fresh fermentation medium and 35 g/L glucose (Fig. 7a). An increased iron concentration has been reported to be favorable for improving heme production [15], 200 mg/L of $FeSO_4{\cdot}7H_2O$ was used in fed-batch fermentation. A total ICPDs titer of was reached 1592 ± 52 mg/L with an extracellular ICPDs secretion rate of 45.5% at 28 h of fed-batch fermentation (Fig. 7b). The ICPDs productivity was 56.86 mg/L/h. Given the limitation of the heme fluorescence assay [45], HPLC analysis was used to determine the heme production. The heme production of HS12 was 98.9 ± 2.4 mg/L with an extracellular heme secretion rate of 46.4% at 28 h of fed-batch fermentation (Fig. 7c). These results suggested that the engineered strain HS12 should be a promising microbial cell factory for industrial heme production.

In recent years, many reports have been published on the production of porphyrin derivatives in *C. glutamicum* by metabolic engineering. A recurring challenge in these studies was the intricate regulation of the porphyrin derivatives biosynthetic pathway in *C. glutamicum*. In previous studies, attempts had been made to improve heme production by altering the arrangement of key genes on the plasmid [23], overexpressing iron metabolism-related transcriptional regulators [19], and replacing the key genes with exogenous genes [22]. In this study, a novel pathway which had not been previously attempted in prokaryotic cells was chosen for efficient heme production. In order to enhance heme biosynthesis, further strategies should be performed in *C. glutamicum*, such as in-depth revelation of the regulatory mechanisms of endogenous pathway, clarification of the rate-limiting steps of the heme production process, and fine tuning of the expression of key genes.

4. Conclusions

In this study, a highly efficient *C. glutamicum* chassis for heme production was constructed by modularizing of complex heme synthetic pathways and finely regulating the expression of each module. Our study showed that the SHD pathway was the optimal heme synthetic pathway for heme production in *C. glutamicum* for the first time. Coordinated expression of key genes in UPG III synthetic module and heme synthetic module was proved to be essential for heme accumulation. The best-performing strain, HS12, produced 421 mg/L ICPDs in a shake flask and 1592 mg/L in a 5 L fed-batch fermenter, underscoring its promise as a heme and other porphyrins production strain.

Funding

This work was financially supported by the National Key Research and Development Program of China, China (2021YFC2100700) and the National Natural Science Foundation of China, China (NSFC-22278312).

Data availability statement

No new data were created.

CRediT authorship contribution statement

Qiuyu Yang: Writing – original draft. **Xi Sun:** Writing – original draft. **Hong Wang:** Writing – original draft. **Tao Chen:** Writing – review & editing. **Zhiwen Wang:** Conceptualization, Supervision, All authors have read and agreed to the published version of the manuscript.

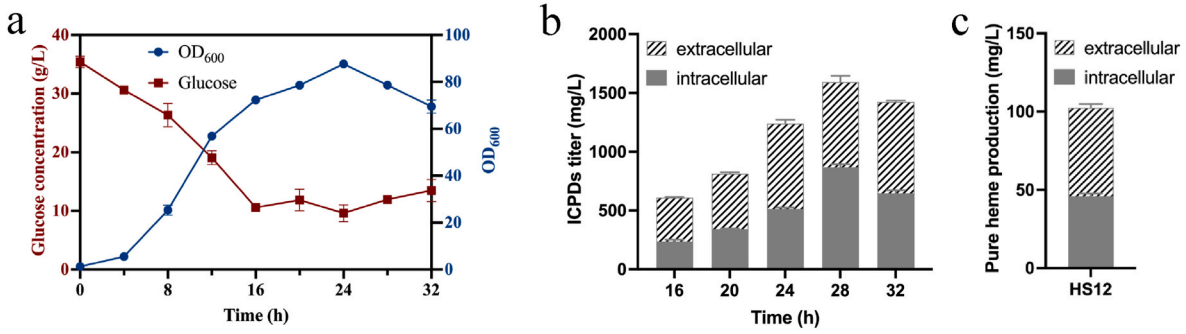

Fig. 7. Fed-batch fermentation of HS12. a, Cell growth and glucose consumption of HS12. b, ICPDs production of HS12. c, heme production of HS12 at 28 h in fed-batch fermentation.

Declaration of competing interest

The authors declare that they have no known competing financial interests or personal relationships that could have appeared to influence the work reported in this paper.

Appendix A. Supplementary data

Supplementary data to this article can be found online at https://doi.org/10.1016/j.synbio.2024.02.008.

References

[1] Li Y, Zhang L. The chemical and structural bases of heme recognition: binding interactions of heme with proteins and peptides. In: Heme biology. WORLD SCIENTIFIC; 2011. p. 161–96.

[2] Lee J, Yesilkanal AE, Wynne JP, Frankenberger C, Liu J, Yan J, et al. Effective breast cancer combination therapy targeting BACH1 and mitochondrial metabolism. Nature 2019;568:254–8. https://doi.org/10.1038/s41586-019-1005-x.

[3] Anderson KE, Collins SD. 192 hemin treatment for acute porphyria: implications for clinical practice of an open-label study of 130 patients. J Invest Med 2006;54:S290. https://doi.org/10.1016/j.amjmed.2006.05.026.

[4] Waltz E. Appetite grows for biotech foods with health benefits. Nat Biotechnol 2019;37:573–5. https://doi.org/10.1038/d41587-019-00012-9.

[5] Zhang J, Cui Z, Zhu Y, Zhu Z, Qi Q, Wang Q. Recent advances in microbial production of high-value compounds in the tetrapyrrole biosynthesis pathway. Biotechnol Adv 2022;55:107904. https://doi.org/10.1016/j.biotechadv.2021.107904.

[6] Schmitz LM, Rosenthal K, Lutz S. Recent advances in heme biocatalysis engineering. Biotechnol Bioeng 2019;116:3469–75. https://doi.org/10.1002/bit.27156.

[7] Fischer H, Zeile K. Synthese des hmatoporphyrins, protoporphyrins und hmins. Eur J Org Chem 2010;468:98–116. https://doi.org/10.1002/jlac.19294680104.

[8] Espinas NA, Kobayashi K, Takahashi S, Mochizuki N, Masuda T. Evaluation of unbound free heme in plant cells by differential acetone extraction. Plant Cell Physiol 2012;53:1344–54. https://doi.org/10.1093/pcp/pcs067.

[9] Yang Q, Zhao J, Zheng Y, Chen T, Wang Z. Microbial synthesis of heme b: biosynthetic pathways, current strategies, detection, and future prospects. Molecules 2023;28(8):3633.

[10] Kaufholz AL, Hunter GA, Ferreira GC, Lendrihas T, Hering V, Layer G, et al. Aminolaevulinic acid synthase of Rhodobacter capsulatus: high-resolution kinetic investigation of the structural basis for substrate binding and catalysis. Biochem J 2013;451:205–16. https://doi.org/10.1042/BJ20121041.

[11] Dailey HA, Dailey TA, Gerdes S, Jahn D, Jahn M, O'Brian MR, Warren MJ. Prokaryotic heme biosynthesis: multiple pathways to a common essential product. Microbiol Mol Biol Rev 2017;81. https://doi.org/10.1128/MMBR.00048-16.

[12] Bali S, Lawrence AD, Lobo SA, Saraiva LM, Golding BT, Palmer DJ, et al. Molecular hijacking of siroheme for the synthesis of heme and d_1 heme. Proc Natl Acad Sci USA 2011;108:18260–5. https://doi.org/10.1073/pnas.1108228108.

[13] Kwon SJ, de Boer AL, Petri R, Schmidt-Dannert C. High-level production of porphyrins in metabolically engineered Escherichia coli: systematic extension of a pathway assembled from overexpressed genes involved in heme biosynthesis. Appl Environ Microbiol 2003;69:4875–83. https://doi.org/10.1128/AEM.69.8.4875-4883.2003.

[14] Zhao XR, Choi KR, Lee SY. Metabolic engineering of *Escherichia coli* for secretory production of free haem. Nat Catal 2018;1:720–8. https://doi.org/10.1038/s41929-018-0126-1.

[15] Choi KR, Yu HE, Lee H, Lee SY. Improved production of heme using metabolically engineered *Escherichia coli*. Biotechnol Bioeng 2022;119:3178–93. https://doi.org/10.1002/bit.28194.

[16] Ikeda M, Nakagawa S. The *Corynebacterium glutamicum* genome: features and impacts on biotechnological processes. Appl Microbiol Biotechnol 2003;62:99–109. https://doi.org/10.1007/s00253-003-1328-1.

[17] Zha J, Zhao Z, Xiao Z, Eng T, Mukhopadhyay A, Koffas MA, Tang YJ. Biosystem design of *Corynebacterium glutamicum* for bioproduction. Curr Opin Biotechnol 2023;79:102870. https://doi.org/10.1016/j.copbio.2022.102870.

[18] Chai M, Deng C, Chen Q, Lu W, Liu Y, Li J, et al. Synthetic biology toolkits and metabolic engineering applied in *Corynebacterium glutamicum* for biomanufacturing. ACS Synth Biol 2021;10:3237–50. https://doi.org/10.1021/acssynbio.1c00355.

[19] Ko YJ, Kim M, You SK, Shin SK, Chang J, Choi HJ, et al. Animal-free heme production for artificial meat in Corynebacterium glutamicum via systems metabolic and membrane engineering. Metab Eng 2021;66:217–28. https://doi.org/10.1016/j.ymben.2021.04.013.

[20] Wang M, Shi Z, Gao N, Zhou Y, Ni X, Chen J, et al. Sustainable and high-level microbial production of plant hemoglobin in *Corynebacterium glutamicum*. Biotechnol Biofuels Bioprod 2023;16:80. https://doi.org/10.1186/s13068-023-02337-9.

[21] Zhang C, Li Y, Zhu F, Li Z, Lu N, Li Y, et al. Metabolic engineering of an auto-regulated Corynebacterium glutamicum chassis for biosynthesis of 5-aminolevulinic acid. Bioresour Technol 2020;318:124064. https://doi.org/10.1016/j.biortech.2020.124064.

[22] Yu X, Jin H, Liu W, Wang Q, Qi Q. Engineering Corynebacterium glutamicum to produce 5-aminolevulinic acid from glucose. Microb Cell Factories 2015;14:183. https://doi.org/10.1186/s12934-015-0364-8.

[23] Seok J, Ko YJ, Lee ME, Hyeon JE, Han SO. Systems metabolic engineering of Corynebacterium glutamicum for the bioproduction of biliverdin via protoporphyrin independent pathway. J Biol Eng 2019;13:28. https://doi.org/10.1186/s13036-019-0156-5.

[24] Zhou Y, Chen J, Pu W, Cai N, Che B, Yang J, et al. Development of a growth-coupled selection platform for directed evolution of heme biosynthetic enzymes in *Corynebacterium glutamicum*. Front Bioeng Biotechnol 2023;11:1236118. https://doi.org/10.3389/fbioe.2023.1236118.

[25] Frunzke J, Gatgens C, Brocker M, Bott M. Control of heme homeostasis in Corynebacterium glutamicum by the two-component system HrrSA. J Bacteriol 2011;193:1212–21. https://doi.org/10.1128/JB.01130-10.

[26] Ko YJ, Joo YC, Hyeon JE, Lee E, Lee ME, Seok J, et al. Biosynthesis of organic photosensitizer Zn-porphyrin by diphtheria toxin repressor (DtxR)-mediated global upregulation of engineered heme biosynthesis pathway in Corynebacterium glutamicum. Sci Rep 2018;8:14460. https://doi.org/10.1038/s41598-018-32854-9.

[27] Sun X, Mao Y, Luo J, Liu P, Jiang M, He G, et al. Global cellular metabolic rewiring adapts *Corynebacterium glutamicum* to efficient nonnatural xylose utilization. Appl Environ Microbiol 2022;88:e0151822. https://doi.org/10.1128/aem.01518-22.

[28] Breinig S, Kervinen J, Stith L, Wasson AS, Fairman R, Wlodawer A, et al. Control of tetrapyrrole biosynthesis by alternate quaternary forms of porphobilinogen synthase. Nat Struct Biol 2003;10:757–63. https://doi.org/10.1038/nsb963.

[29] Jordan PM. Chapter 1 the biosynthesis of 5-aminolaevulinic acid and its transformation into uroporphyrinogen III. N Compr Biochem 1991;19:1–66. https://doi.org/10.1016/S0167-7306(08)60108-8.

[30] Silva PJ, Ramos MJ. Comparative density functional study of models for the reaction mechanism of uroporphyrinogen III synthase. J Phys Chem B 2008;112:3144–8.

[31] Tian Q, Li T, Hou W, Zheng J, Schrum LW, Bonkovsky HL. Lon peptidase 1 (LONP1)-dependent breakdown of mitochondrial 5-aminolevulinic acid synthase protein by heme in human liver cells. J Biol Chem 2011;286:26424–30. https://doi.org/10.1074/jbc.M110.215772.

[32] Kitatsuji C, Ogura M, Uchida T, Ishimori K, Aono S. Molecular mechanism for heme-mediated inhibition of 5-aminolevulinic acid synthase 1. Bull Chem Soc Jpn 2014;87:997–1004. https://doi.org/10.1246/bcsj.20140111.

[33] Ishikawa H, Nakagaki M, Bamba A, Uchida T, Hori H, O'Brian MR, et al. Unusual heme binding in the bacterial iron response regulator protein: spectral characterization of heme binding to the heme regulatory motif. Biochemistry 2011;50:1016–22. https://doi.org/10.1021/bi101895r.

[34] He G, Jiang M, Cui Z, Sun X, Chen T, Wang Z. Construction of 5-aminolevulinic acid synthase variants by cysteine-targeted mutation to release heme inhibition. J Biosci Bioeng 2022;134:416–23. https://doi.org/10.1016/j.jbiosc.2022.07.019.

[35] Bali S, Lawrence AD, Lobo SA, Saraiva LM, Golding BT, Palmer DJ, et al. Molecular hijacking of siroheme for the synthesis of heme and d1 heme. Proc Natl Acad Sci U S A 2011;108:18260–5. https://doi.org/10.1073/pnas.1108228108.

[36] Mardanov AV, Sorokin DY, Beletsky AV, Ravin NV. Complete genome sequence of "*Candidatus Syntrophocurvum alkaliphilum*" strain B(2M), obtained from the metagenome of a salt-tolerant Alkaliphilic anaerobic syntrophic butyrate-degrading consortium. Microbiol Resour Announc 2020;9. https://doi.org/10.1128/MRA.01511-19.

[37] Dailey HA, Gerdes S, Dailey TA, Burch JS, Phillips JD. Noncanonical coproporphyrin-dependent bacterial heme biosynthesis pathway that does not use protoporphyrin. Proc Natl Acad Sci USA 2015;112:2210–5. https://doi.org/10.1073/pnas.1416285112.

[38] Jiang P, Fang H, Zhao J, Dong H, Jin Z, Zhang D. Optimization of hydrogenobyrinic acid biosynthesis in Escherichia coli using multi-level metabolic engineering strategies. Microb Cell Factories 2020;19:118. https://doi.org/10.1186/s12934-020-01377-2.

[39] Yang S, Wang A, Li J, Shao Y, Sun F, Li S, et al. Improved biosynthesis of heme in *Bacillus subtilis* through metabolic engineering assisted fed-batch fermentation. Microb Cell Factories 2023;22:102. https://doi.org/10.1186/s12934-023-02077-3.

[40] Allen CE, Schmitt MP. HtaA is an iron-regulated hemin binding protein involved in the utilization of heme iron in Corynebacterium diphtheriae. J Bacteriol 2009;191:2638–48. https://doi.org/10.1128/JB.01784-08.

[41] Keppel M, Davoudi E, Gatgens C, Frunzke J. Membrane topology and heme binding of the histidine kinases HrrS and ChrS in *Corynebacterium glutamicum*. Front Microbiol 2018;9:183. https://doi.org/10.3389/fmicb.2018.00183.

[42] Wang M, Wang Y, Wang M, Liu M, Cheng A. Heme acquisition and tolerance in Gram-positive model bacteria: an orchestrated balance. Heliyon 2023;9:e18233. https://doi.org/10.1016/j.heliyon.2023.e18233.

[43] Keppel M, Hunnefeld M, Filipchyk A, Viets U, Davoudi CF, Kruger A, et al. HrrSA orchestrates a systemic response to heme and determines prioritization of terminal cytochrome oxidase expression. Nucleic Acids Res 2020;48:6547–62. https://doi.org/10.1093/nar/gkaa415.

[44] Burgos JM, Schmitt MP. The ChrSA and HrrSA two-component systems are required for transcriptional regulation of the hemA promoter in *Corynebacterium diphtheriae*. J Bacteriol 2016;198:2419–30. https://doi.org/10.1128/JB.00339-16.

[45] Sinclair PR, Gorman N, Jacobs JM. Measurement of heme concentration. Curr Protoc Toxicol 2001. https://doi.org/10.1002/0471140856.tx0803s00 [Chapter 8]:Unit 8 3.